Restoration of transpression/transtension by generating the three-dimensional segmented helical loci of deformed lines across structure contour maps

Angus M. McCoss*

Department of Geology, The Queen's University of Belfast, Belfast BT7 1NN, Northern Ireland

Abstract—In transpression/transtension zones the strain is three-dimensional and rotational. This causes material to move through the plane of cross-section, often invalidating balancing and restoration within this plane. Methods are presented which allow the three-dimensional segmented, irregular, helical locus of an originally straight line to be constructed, in any direction, on a structure contour map of a folded and faulted surface. This construction depends on a knowledge of the kinematics of folding and faulting and can be modified to suit local conditions. The ratio of the length of the cylindrical envelope bounding this helical locus, to the sum of the lengths of the helical fragments between faults, gives the true stretch in the direction of the envelope. When the traces of the segmented helices are constructed in different directions on a deformed surface, the sectional finite-strain ellipse can be found for that surface. Knowledge of the dimensions of this ellipse and its orientation with respect to the kinematic axes of the transpression zone allows the tensor components to be constrained. This permits the three-dimensional boundary conditions to be determined and thus restored.

The methods are applied to the Ardross Fault zone in central Scotland. The solutions suggest this fault zone underwent a phase of dextral transpression along a NW zone boundary during Hercynian E–W compression in the Scottish Midland Valley. Contemporaneous E–W dyke swarms and N–S regional flexures support these kinematics.

INTRODUCTION

RESTORATIONS of thrust belts and extensional basins are usually achieved by reconstructing cross-sections in the plane containing the bulk displacement vector; movements of material through this plane are generally not considered. If, however, the deformation is triaxial and rotational, as it is in transpression/transtension, then in general section planes will have movement of material through them.

For this reason the deformation represented in two-dimensional cross-sections through triaxially deformed rocks cannot be restored directly. Instead, a three-dimensional representation of the deformation must be restored. Barr (1984a,b, 1985) recognized this and proposed that structure contour maps should be restored in non-plane strain deformations. His valuable work in this field is, however, limited to basins in which the most significant component of the bulk deformation is attributable to faulting. Although he considered the effects of hangingwall rollover anticlines, folding in general was not fully considered. Furthermore the restorations he presented assume very simple fault kinematics; for example, slip vectors of all faults in a basin have parallel map projections; all faults are dip-slip; or slip vectors of all faults have map projections which lie normal to the axes of their 'rollover' anticlines (Barr 1985).

This paper introduces a new technique for restoring structure contour maps of horizons folded and faulted in

triaxial strains, and this technique is particularly suitable for the analysis of transpression/transtension. It involves measuring the bulk finite sectional strain ellipse in the plane of regional bedding (the first-order trend surface representing the deformed horizon). This sectional strain ellipse is measured by considering two three-dimensional components of the deformation; faulting and folding. If the sectional ellipse is orientated with respect to principal or kinematic axes it can then be used to constrain the triaxial deformation, in this case represented by the transpression tensor of Sanderson & Marchini (1984). Knowledge of a tensor which could generate the observed strain facilitates a description of the possible boundary conditions, which can then be restored. Furthermore, the inverse tensor, or reciprocal deformation, can restore not only the boundaries but also regional geological features to their former attitudes.

The presented methods have been developed to allow a reconstruction of the deformation associated with the Ardross Fault, a Hercynian dextral wrench fault in the Scottish Midland Valley (Fig. 1). Although the example is of a relatively small volume of rock (about 10^7 m^3), the methods are essentially independent of scale and could be used with larger-scale structure contour maps. (These maps could be seismically derived or generated from field observations.)

Assumptions are made about the kinematics of structures which, although applicable to the Ardross Fault zone, may require modification in other situations. Several alternative strategies are suggested, but it is the general approach to the restoration of zones in which horizons have been folded and faulted in triaxial deformations that is emphasized here.

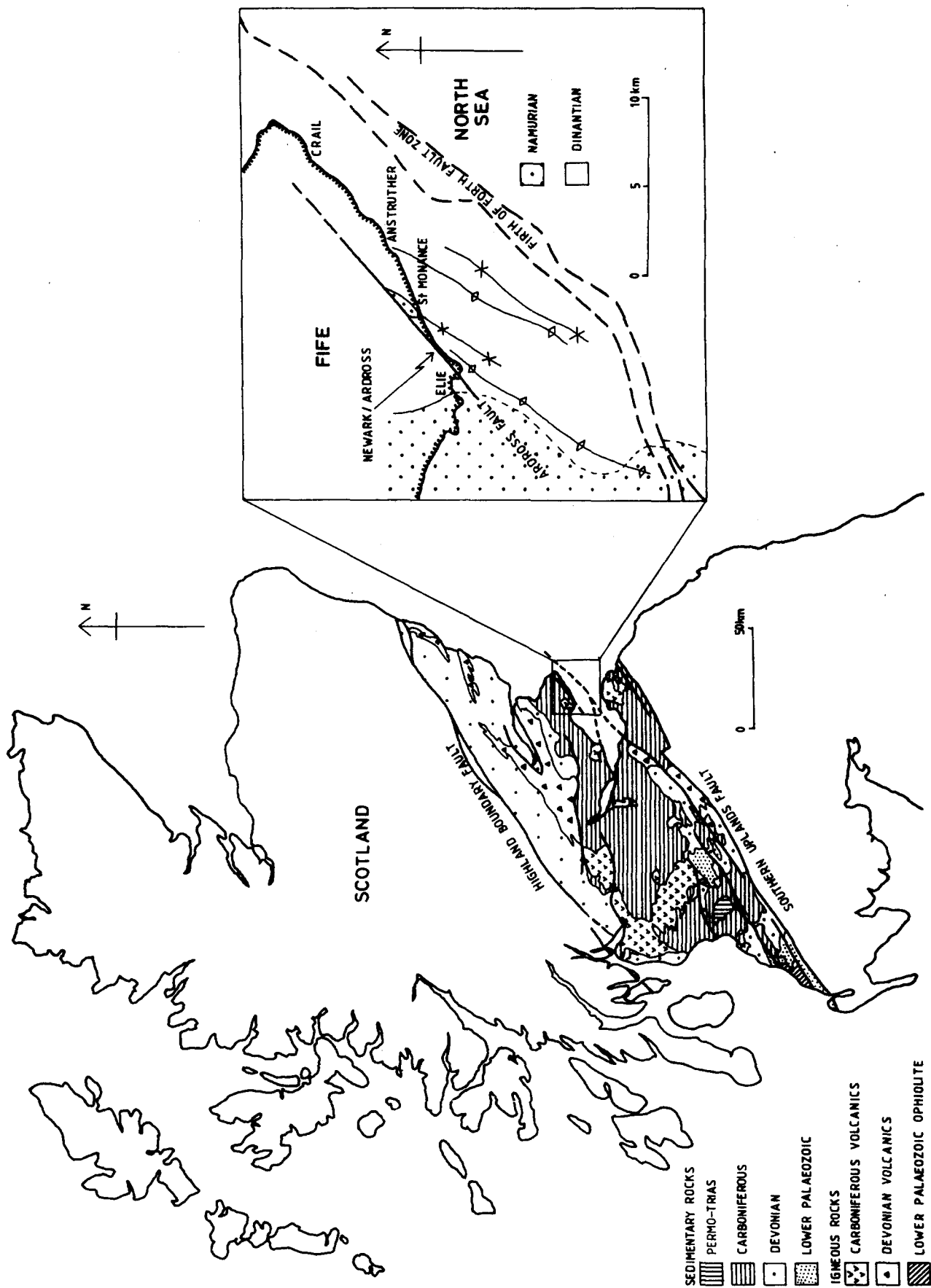*Present address: Shell Internationale Petroleum Maatschappij, Oostduinlaan 75, 2596JJ, The Hague, The Netherlands.

Fig. 1. Location map of the Ardross Fault zone in the Scottish Midland Valley.

THREE-DIMENSIONAL STRAINS RESULTING FROM FAULTING

Structure contour maps of deformed horizons are commonly used by exploration geologists and are usually seismically derived. They can also be drawn by extrapolation of data from a geologically mapped surface. Besides representing a folded surface, contour maps usually contain the lenticular projections of the hanging-wall and footwall cut-offs of the faults which intersect that surface. In the following discussion these are called the 'cut-off lenses'. Further to this, the geologist may have been able to constrain the probable slip directions on these faults, in which case the map projections of the slip vectors could be superimposed on the cut-off lenses.

The bulk strain in any direction in a contour map containing this information can be found by drawing a line across the map in any desired direction until it intersects a fault cut-off lens (Fig. 2). At this point the course of the line should be deflected parallel to the map projection of the slip vector. Upon reaching the opposite side of the cut-off lens, the line should resume its original trend until reaching the next cut-off, where it should again be 'dog-legged' along the map projection of the slip vector, and so on across the rest of the map.

This dog-legged line across the structure contour map now records the strain measured both in a vertical plane (using the elevations from the contours), and in a horizontal plane (using the positions in the map). In other words, the segmented and dog-legged line records the strain in three dimensions. The stretch (measured in the direction of the cylindrical envelope bounding this segmented line) is determined by dividing the length of the envelope by the sum of the lengths of the line fragments between the faults (Fig. 3). Note that all these lengths should be measured in three dimensions using the positions and elevations from the structure contour map.

EXTRAPOLATION ONTO CONTOUR MAPS

To measure the three-dimensional strains resulting from faulting, a knowledge of the cut-off lenses and slip

vectors is obviously required. Unfortunately they are both notoriously difficult to determine. Three-dimensional seismic surveying helps constrain cut-off lenses, but for the field geologist other practical strategies are required. As for constraining slip vectors, the seismic interpreter cannot resolve features such as slickenside lineations. Even the field geologist finds that slickenside lineations often only mark a component of net slip, and that lithological piercements are sparse. Tectonic piercements, such as fold hinges, are particularly valuable where there is no ambiguity in matching pre-existing hinges. However, fault traces are often shorter than the fold wavelength, leaving only map separations (of bedding traces and contour lines), bedding attitude and fault attitude as attainable data.

The following two sections suggest ways in which this attainable data can be used objectively to generate representative cut-off lenses and slip vectors on contour maps. These strategies, like most extrapolative techniques, have their limitations and the geologist may prefer to define his or her own for a given situation. What is important, however, is that cut-off lenses and slip vectors must be represented on the contour map if the component of the bulk strain attributable to faulting is to be considered.

A simple method for determining slip vectors from bedding attitude, fault attitude and map separation (of bedding traces or contour lines)

One set of the three commonly measurable quantities: bedding attitude, fault attitude and sense of map separation of bedding traces (or contour lines), does not give a unique solution for the slip vector of a fault. If, however, (1) the faults can be divided into sub-parallel sets, (2) the faults in a set have sub-parallel slip vectors and (3) the bedding is variably dipping, then slip vectors can be assigned to each fault set. This is achieved for a set of faults by plotting their intersections with bedding on a stereogram and assigning them an appropriate dextral or sinistral map-separation symbol (Fig. 4). The resulting stereogram depicts a great circle spread in which the sinistral and dextral separation symbols lie on either side of the slip vector. It should be emphasized that this technique can also be used directly on seismically-derived contour maps by using the map separations of contours (of the same elevation) in place of bedding traces on the geological map.
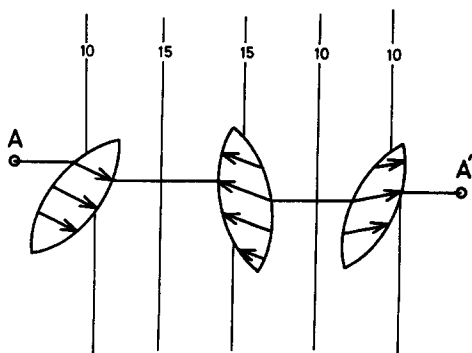
Fig. 2. Contour map of a gently flexured sub-horizontal layer cut by oblique faults of finite areal extent. The lenticular outlines are the hangingwall and footwall cutoffs ('cut-off lenses'). The arrows are the map projections of the slip vectors, and the dog-legged trace AA' represents the trace of an originally straight line on the pre-faulting bedding surface.
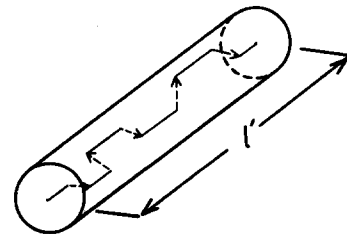
Fig. 3. The cylindrical envelope bounding a line which is segmented in three dimensions by movements on faults. The fault slip vectors are represented by the dashed arrows. The stretch in the direction of the envelope is simply the length, l', of the envelope, divided by $\Sigma\, l_0$, the sum of the line fragments (solid lines) between the faults.
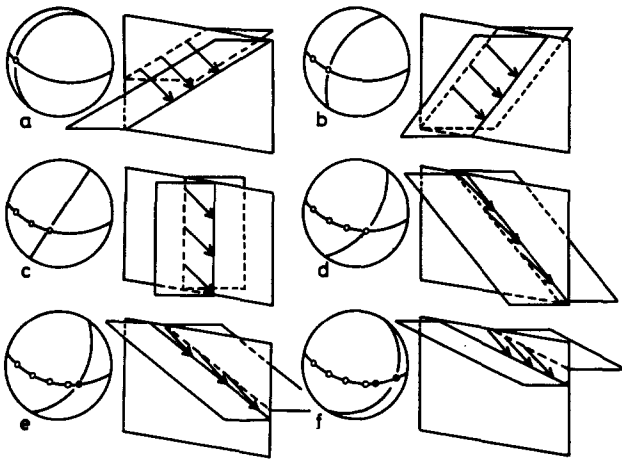
Fig. 4. Method for determining slip vectors from observations of bedding separations. The slip vectors (heavy arrows) in the fault plane generate sinistral (open circles) or dextral (solid circles) map separations depending on the orientation of the bedding-fault intersection. (a)–(f) depict a rotation of the intersection from west-plunging through down-fault dip to east-plunging. Note that once the intersection passes through the slip vector, the sense of map separation changes. The orientation at which this change occurs can thus be used as an approximation of the slip vector for a set of sub-parallel faults.

This technique would probably not apply to the traces of anastomosing wrench zones where dip-slip and wrench faults are often sub-parallel. In such cases combinations of the standard methods for determining slip vectors would have to be used (e.g. slickensides and lithological piercements). What is important, however, is that the slip vectors of the faults must be known, or at least constrained, to restore transpression or any other triaxial deformation.

Utilizing data at the geologically-mapped surface to determine a representative population of fault cut-off lenses in a structure contour map

Having obtained the directions of the slip vectors, the magnitude of displacement can be defined from the distance between the hangingwall and footwall cut-offs in this direction. These cut-offs may be relatively easy to determine from three-dimensional seismic surveys, but for the field geologist they are more problematical. A simple objective strategy has therefore been developed for the field geologist to utilize the information gathered at the geologically mapped surface. This strategy could also be modified to suit individual requirements.

In areas where finite fault traces are mapped at the surface we are faced with the problem of projecting them to depth. If it is assumed that the tip-line of the fault is sub-elliptical, then the fault trace at the surface is simply a chord to that ellipse. To be able to project individual faults onto a contour map, we would need to know the relative positions of the contoured horizon and the tip-line ellipses. Even knowing the tip-line geometry of surface faults, we would generally find that the contour map would have fewer faults than the surface map, because of the finite areal extent of the faults. Clearly this would be a misrepresentation of the deformation, since the contoured horizon would probably be inter-

sected by other faults whose tip-lines did not reach the mapped surface.

In an attempt to account for the bulk strain attributable to faulting we could assume that the contour map and the surface map have similar fault populations. This approach is particularly applicable where faults have short traces and tend to be steep, isolated from one another and uniformly distributed throughout the body of rock. If, however, there is evidence of a horizontal detachment, it would be unreasonable to project the fault population beneath it. The following discussion assumes that the surface map and the contour map have similar fault populations and that the strain attributable to faulting in one is equivalent to that in the other.

There are two obvious strategies for projecting the faults onto the contour map. Either the tip-line ellipse is projected down the fault dip to the contour map, describing a planar strip, or it is moved vertically onto it, describing an elliptical cylinder. Since the projections are done simply to generate a representative distribution of faults on the contour map, and not to locate individual faults, it does not matter which strategy is adopted. However, to preserve the spatial relationships of faulting and folding, measured on the surface geology map, vertical projection of faults onto the contour map is preferred.

To ensure that the strain attributable to faulting is the same in both maps, an objective strategy must be defined for determining the dimensions of the fault cut-off lenses. The information we would generally have at our disposal from the surface geology map (Fig. 5a) would be as follows: (1) TT', the length of the fault trace; (2) M, the position of the point of maximum apparent separation; (3) BB', the magnitude of this maximum apparent separation; (4) the orientation of the fault; (5) the orientation of bedding at M; (6) the orientation of the contoured horizon, H–H', directly below the point M.

Conservation of the area of the cut-off lens (measured in the fault plane) effectively ensures that the strain attributable to faulting is the same in both the surface geology map and the contour map. Furthermore, it is taken that a fault plane represented in the surface geology map is parallel to its projected equivalent in the contour map. Thus cut-off lens area will not only be conserved in the plane of the fault, but will also be conserved in the map plane. This permits the dimensions of a cut-off lens, determined in the surface geology map, to be used to construct a similar cut-off lens in the contour map.

The procedure for determining the dimensions of a cut-off lens in a surface geology map is outlined in Fig. 5(b). First, draw the two sets of structure contours representing the fault and a bedding-parallel surface through M, and construct the intersection UU' of these two surfaces. The trace of UU' is parallel to the map projection of the long axis of the fault cut-off lens in the surface geology map. It is taken that (on average) the length of the long axis, CC', is equal to the length of the fault trace TT'. (This assumption is made because,
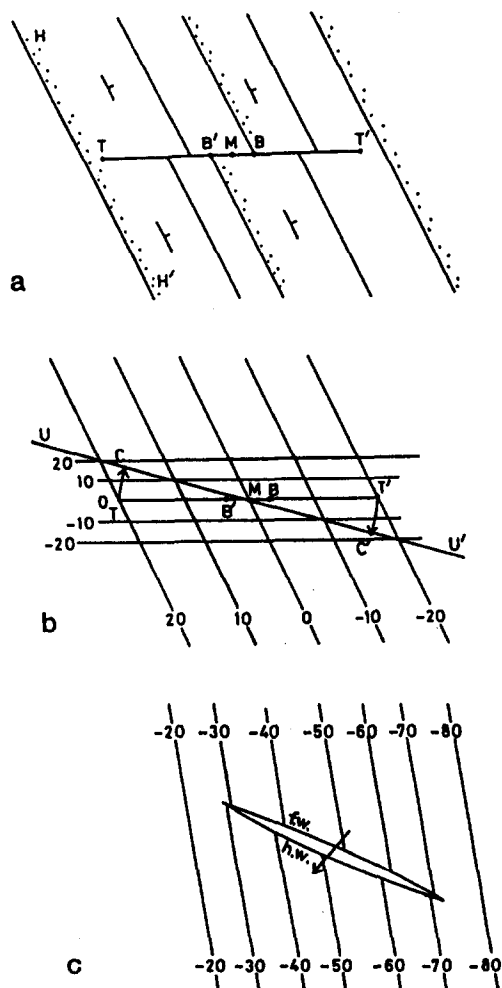
Fig. 5. Procedure for determining fault cut-offs on a structure contour map. See text for details.

the surface map is adequately represented in the contour map. Indeed the user is free to define his own strategies. What is important, however, is that the strain attributable to faulting should be constrained as well as is practically possible, whether or not this includes extrapolation.

THREE-DIMENSIONAL STRAINS RESULTING FROM FOLDING

When folded, originally straight lines on bedding surfaces in general become irregular, three-dimensional helices, or in special cases inclined planar curves (see Ramsay 1967, Chapter 8-3). The map projections of these deformed traces are not straight lines. This implies that there must, in general, be a map-plane deformation associated with folding. Only in a few special cases does the deformed line become a vertical planar curve, and only then should it be restored in that plane. In general, however, it is the three-dimensional helical loci of deformed lines which should be restored. Unfortunately, kilometre-scale deformed lines are rare in nature (!) so they must be generated across a contour map.

A full discussion of the deformation of lineations by folding is given in Ramsay (1967, Chapter 8). However a more detailed study of the effect of flexural-slip folding on the three-dimensional movement of material is now considered, both because it is a simple model and because it is applicable in many non-metamorphic zones of deformation. Other folding models could equally well be applied, using the appropriate loci of deformed lineations in a manner similar to that outlined below.

without knowledge of the position of the tip-line, it is equally likely that CC' could be slightly longer or slightly shorter than TT'.) Having constrained the orientation and length of the map view of the cut-off lens, its width can be effectively constrained by the points B and B' which delimit the maximum separation at the surface. The four points C, B, C' and B', constrain the dimensions of the cut-off lens, which should be drawn on the contour map.

Although the outline, and thus area, of the cut-off lens is directly transferred to the contour map, it will probably need to be rotated. This is because, in general, the attitude of bedding at the surface will not be equal to that at a point directly below on the contour map. The desired orientation of the long axis of the cut-off lens in the contour map is determined using the intersection of the fault and bedding contours in a manner similar to that shown in Fig. 5(b). The map projection of the slip vector can then be superimposed and contouring can be completed up to the edges of the lens (Fig. 5c), making sure that the magnitudes of slip are compatible with those determined at the surface.

It must be emphasized that the above procedures do not claim to locate the positions and dimensions of faults at depth, they simply attempt to ensure that the strain in

Generating the traces of the helical loci of deformed lines across structure contour maps

A straight line in a surface will, on folding, form a helix that has a geometry dependent on the fold mechanism. For flexural-slip folds the line will have a constant angular relationship with the fold axis (Ramsay 1967, p. 463), and its locus will plot as a partial small-circle on a stereogram. This permits the three-dimensional configuration of the trace to be easily constructed across a structure contour map. It can then be measured and used to calculate the component of the strain attributable to folding.

The method for determining the trace of the helical locus, $i_0 i_N$, across the contour map is illustrated in Fig. 6 and is described as follows.

(1) Determine the local fold axis, β, from the contour map and/or measurements made at the mapped surface and plot it on a stereogram.

(2) Construct the great circle, b_0, representing the plane whose dip vector is β.

(3) On the contour map, draw a short line from the axial trace in any desired direction, $i_0 i_1$, and measure the angle q_0 between it and the trend of β.
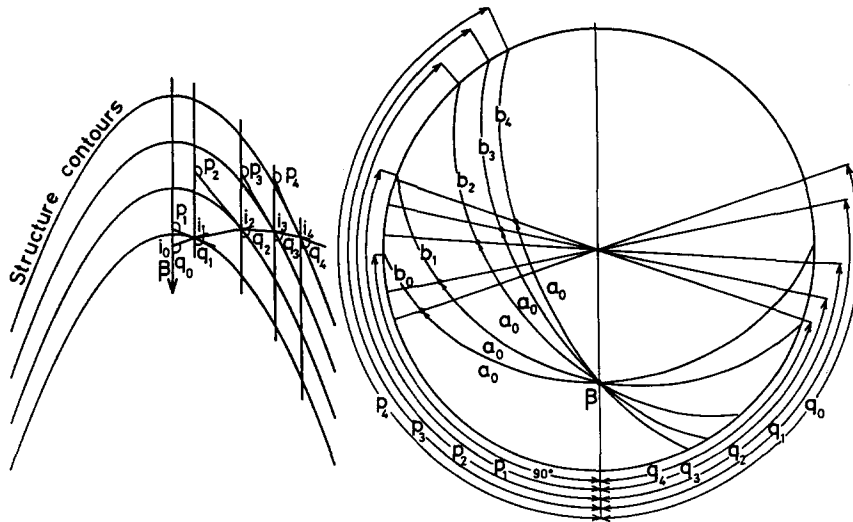
(4) Measure out the horizontal angle q_0 from the

Fig. 6. Diagrammatic representation of the principles for constructing the trace of an originally straight line across a structure contour map where bedding has been folded by flexural-slip. See text for details.

azimuth of β on the stereogram and draw a line which has this trend through the centre of the stereogram.

(5) Determine the point of intersection between this line and b_0.

(6) Measure the angle a_0, from β along b_0 to this intersection point. This is the half-apical angle of the partial small-circle locus of this deformed line.

Knowing the angle a_0, one can determine the map projection of the trace, $i_1 i_N$, of a deformed line across the contour map using the following iterative loop.

(7) On the contour map, at the point i_J, where the short line, $i_{J-1} i_J$, intersects a contour, measure the angle p_J, between the trend of β and the tangent to the contour.

(8) In the horizontal plane, measure out the angle p_J from the azimuth of β on a stereogram and draw the great circle, b_J, which has this strike and passes through β. This great circle represents the bedding at i_J.

(9) Determine the azimuth of the point which lies on the great circle b_J, at an angle a_0 from β. This is the trend of the trace of the deformed line element $i_J i_{J+1}$ across the contour map.

(10) Draw this line element on the contour map until it intersects the next contour at i_{J+1} and return to procedure (7) above.
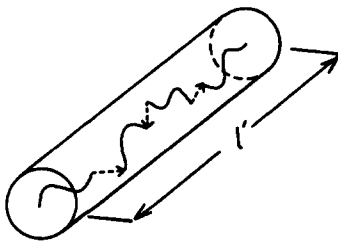
This iterative construction produces a close approximation to the helical trace on the map. Clearly the smoothness of the curve is dependent on the number of iterations per unit length of trace. Any accumulated errors are minimized by generating the traces from their centres, outwards in opposite directions. In order to determine the length, l_0, of the helix, its elevation (from the contour map) is plotted against distance along the map trace, and the length of this curve is measured. The stretch resulting from folding (measured in the direction of the cylindrical envelope bounding the helix) is determined by dividing the length of this envelope by the length, l_0, of the helix.

THREE-DIMENSIONAL STRAINS RESULTING FROM FAULTING AND FOLDING

By combining the above technique for generating helical loci across structure contour maps with the earlier technique of generating the courses of lines which are segmented and dog-legged by fault cut-off lenses, a measure of bulk finite strain can be made. The stretch (measured in the direction of the bounding cylindrical envelope) of the resulting dog-legged helical locus is simply determined by dividing the length, l', of the envelope by $\Sigma\, l_0$, the sum of the lengths of the helical fragments between the faults (Fig. 7). Remember that the lengths should be determined in three-dimensions, using elevation and position on the structure contour map.

Fig. 7. Determination of the bulk linear stretch by dividing the length of the envelope, l', containing the segmented helix by the sum of the component helical segments which lie between the faults (the slip vectors of which are shown as dashed arrows). All measurements are made in three dimensions using position and elevation from a structure contour map.

RESTORING THE BULK FINITE STRAINS

Knowledge of the stretches of the segmented helical loci permits the definition of the bulk finite strain; however, the boundary conditions which lead to that strain cannot be uniquely defined. They can, however, be approximated if a suitable deformation model is

assumed. The constant volume transpression tensor of Sanderson & Marchini (1984) is considered here because it is simple, three-dimensional and general. It can describe the continuous spectrum of deformations which range from plane strain compression in thrust belts, through triaxial transpression, to simple shear in wrench zones, and from there through triaxial transtension, to plane strain extension in basins (see also McCoss 1986).

Perhaps the most convenient way to constrain the components of the transpression tensor is to determine the bulk finite-sectional strain ellipse in the plane of regional bedding. This is achieved by generating segmented helical loci of originally straight lines in different directions across the structure contour map, using the techniques described above. Their stretches are then measured and used to determine the parameters of the rotated ellipse which minimizes the sum of the squares of the residuals (see, for example, Gill & Murray 1978). Since the ellipsoids described by the transpression tensor have a limited set of characteristics it is possible to constrain them with just one sectional ellipse. (A single sectional ellipse can be used to determine the corresponding ellipsoid provided it can be orientated with respect to the principal axes of the ellipsoid, as explained by Ramsay 1967, pp. 148–149, or, as in this case, the kinematic axes of the transpressional deformation.)

In the example below, the kinematic axes of the transpressional deformation are as follows: x is horizontal and parallel to the defined tectonic boundary (the Ardross Fault), y is horizontal but normal to the boundary and z is vertical and parallel to the boundary.

The transpression tensor solution is found by numerical substitution of its components. Substitutions are carried out until the sectional ellipse in a plane parallel to regional bedding (in which the stretches were measured) has the same characteristics as those observed in the measured ellipse. The principal stretches of the measured sectional ellipse are given arbitrary error bars of $\pm 10\%$, and angles are taken as accurate to $\pm 10°$. This facilitates the identification of a suite of probable transpression tensor solutions.

A simple, if somewhat indirect, method for determining the sectional ellipse of an ellipsoid is as follows. First calculate the stretches of three non-parallel lines which pass through the centre of the ellipsoid (see Ramsay 1967, Chapter 4) and also lie in the plane of section. Then use these stretches to constrain the sectional ellipse (see Ramsay 1967, Chapter 3).

RESTORATION OF THE ARDROSS FAULT ZONE

The southeast block of the Ardross Fault, a NE-trending, Hercynian, dextral, wrench fault in the Scottish Midland Valley (Figs. 1, 8 and 9), is used to illustrate the application of the above methods. The Ardross Fault was first described and recognized as a sub-vertical dextral wrench fault by Cumming (1936). Since his work other investigations of the area have been made by Anderson (1951) and Francis & Hopgood (1970). All

but Anderson (pp. 99–100) recognized that the fault has a significant dextral component but disagreed over the magnitude of the displacement.

Of the two fault blocks, the southeastern one is more intensely deformed, comprising closely folded (en échelon) and faulted Lower Carboniferous (Upper Viséan and Lower Namurian) sandstones and shales with subordinate ironstones and limestones. The SE margin of this 7 km-wide block is delineated by the contemporaneous Firth of Forth Fault zone, which trends parallel to the Ardross Fault (Figs. 1 & 9). Since the lengths of these parallel bounding faults are considerably longer than their separation, it is presumed that the rocks deformed in the intervening block were not extruded out of the ends but were instead able to thicken vertically, towards the free surface, between the two steep fault zones. Indeed a measure of the horizontal stretch parallel to the trace of the Ardross Fault (see later) shows that there is no significant strain in this direction, confirming the validity of this assumption.

The fault zone is also intruded by volcanic necks and dykes which were first recognized by Geikie (1879, 1902) and have been dated by their associated pyroclastic deposits elsewhere in Fife as Upper Carboniferous (Namurian and Westphalian) rocks by Francis & Ewing (1961) and Forsyth & Chisolm (1968). Locally, however, Francis (1968) observed that some pyroclastics also occur in the Upper Calciferous Sandstone Measures (Viséan). More recently Forsyth & Rundle (1978) made K–Ar age determinations on the neck intrusions in the area and deduced that they are probably uppermost Carboniferous (Stephanian) or even Permian.

The fault is well exposed on the foreshore at Newark Castle (G.B. National Grid ref. No. 518012), 1 km southwest of St. Monance, Fife, enabling local lithostratigraphic members to be identified and the area subsequently mapped at the scale of 1 : 1000 with the aid of aerial photographs (Fig. 8). The base of the Newark Siltstone member has been selected as a suitable surface for analysis, since its trace is well represented at the mapped surface and it lies near the middle of the stratigraphic sequence. This and the lack of evidence of major horizontal discontinuities make the extrapolation of structures from both above and below more reasonable. The surface was contoured using cubic interpolation to constrain its morphology (McCoss 1987), and then the traces of the fault cut-offs were projected onto it, using the methods described above (Fig. 10). Since the faults generally have short traces, representing isolated and uniformly distributed flaws, the slip vectors were evaluated using the map separation technique (described above), on measurements taken from this and adjacent areas of the southeastern block (Fig. 11). The map components of these slip vectors were then superimposed on the 'cut-off lenses' (Fig. 10). It should be noted that the majority of the faults extend the axial traces of the folds and that these traces trend at low acute angles (anticlockwise) from the trace of the Ardross Fault. These features are predicted in the dextral transpression model of Sanderson & Marchini (1984, fig. 5).

LITHOSTRATIGRAPHIC MEMBERS

NC	NEWARK CASTLE SST.
UA	UPPER ARDROSS
LA	LOWER ARDROSS
UN	UPPER NEWARK
NS	NEWARK SILTSTONE
LN	LOWER NEWARK
UC	UPPER COALYARD

BASALTIC INTRUSIONS

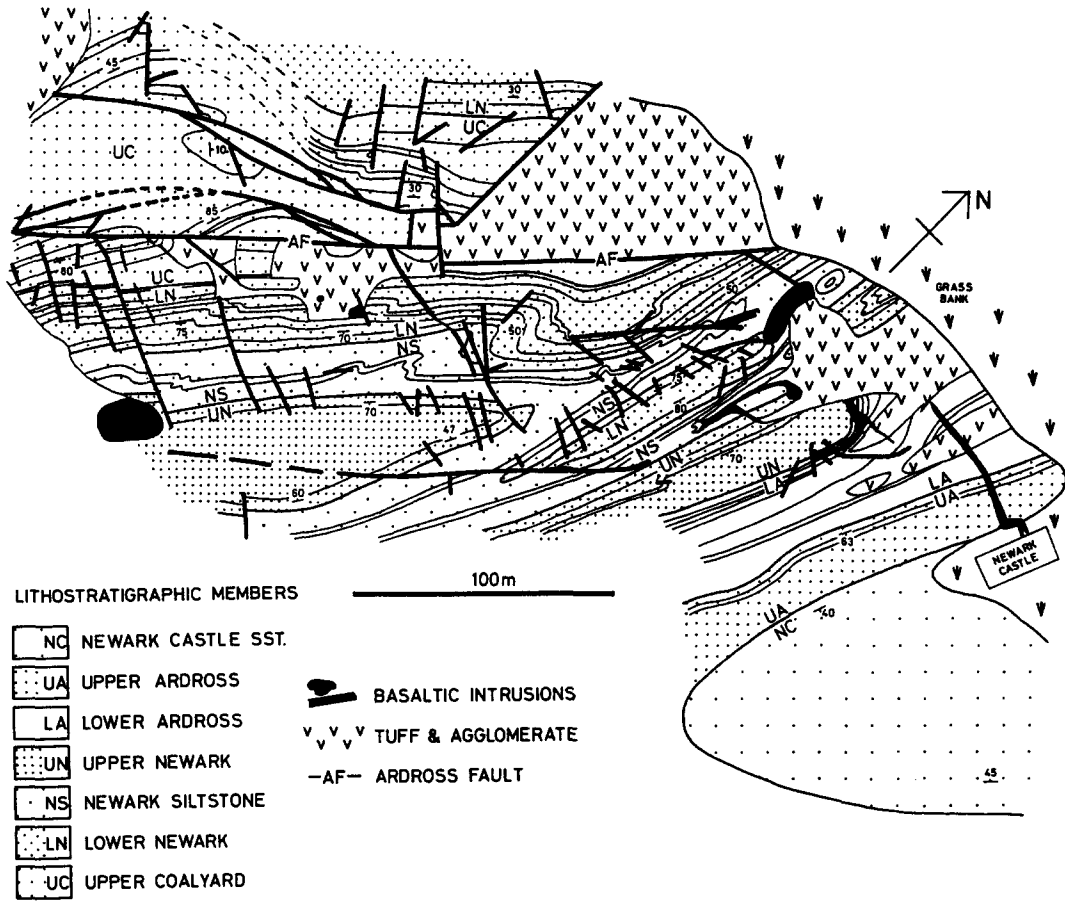$^v_v{}^v_v{}^v$ TUFF & AGGLOMERATE

—AF— ARDROSS FAULT

100m

Fig. 8. Geological map of the Ardross Fault on the foreshore at Newark Castle (Grid ref. NO518012) between St. Monance and Elie, Fife.

Having constructed a representation of the contorted and fractured surface, the segmented helical loci of originally straight lines were generated in five directions across it (Fig. 12). This was achieved using the procedures illustrated in Figs. 2 and 6. A flexural-slip model was adopted as a first approximation for the folding at Newark Castle because the folds are practically parallel and undeformed fossils suggest there is no significant tangential longitudinal strain. The fact that faults extend

the axial traces of the folds does not discount the use of a flexural-slip model, since in this context, it is only used to analyse the segments of the deformed horizon which lie between faults. It is not used to model the large scale geometry of the folds.

After generating the segmented helical loci one can measure the lengths of the cylindrical envelopes bounding them and lying parallel to the plane of regional bedding (which dips at 50° towards 120°). These lengths

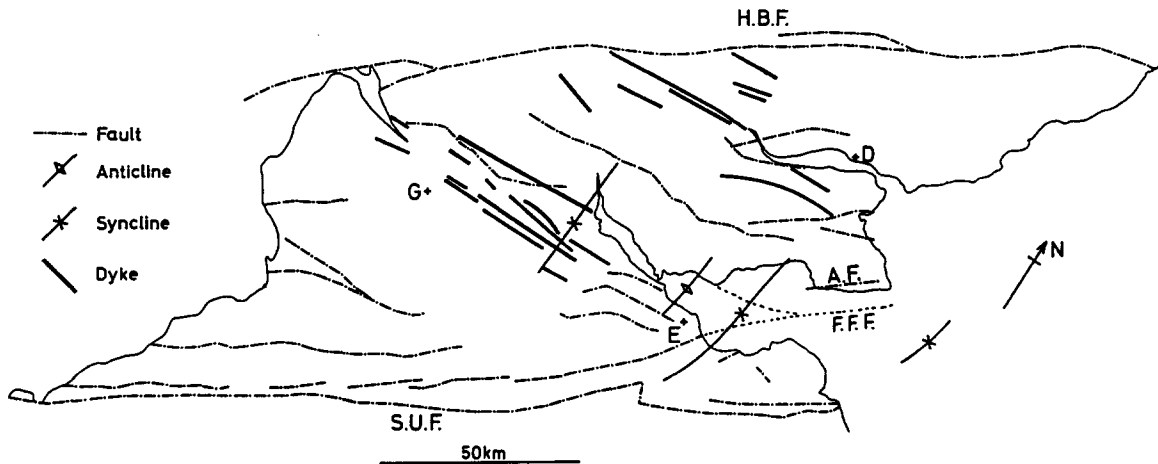— — — Fault

✗ Anticline

✗ Syncline

\ Dyke

50km

Fig. 9. Major structural components in the Scottish Midland Valley which were active during Hercynian tectonics. Abbreviations: A.F., Ardross Fault; F.F.F., Firth of Forth Fault; H.B.F., Highland Boundary Fault; S.U.F., Southern Uplands Fault; E., Edinburgh; G., Glasgow; D., Dundee.
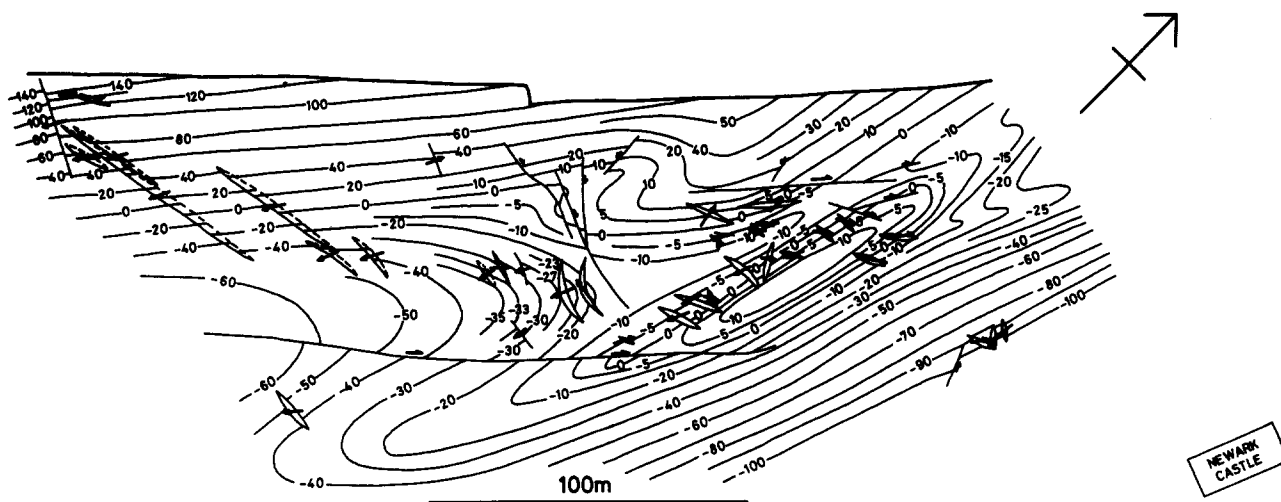
Fig. 10. Structure contour map of the base of the Newark Siltstone member. The 'cut-off lenses' and map components of the slip vectors of the faults are superposed. Contours are in metres.

were then divided by the corresponding sums of the lengths of the individual helical segments between faults to give a measure of the stretch in each of the five directions. The measured stretches are shown in Fig. 13(a) and are used to constrain a least-squares bulk finite strain ellipse in the plane of regional bedding (Fig. 13b). Although there is no line in regional bedding which is exactly horizontal and parallel to the trace of the Ardross Fault (the x axis), the generated locus a is only 12° from

this orientation (see Figs. 12 and 13a). It is significant that the stretch along locus a is only 0.98: this line (sub-parallel to the x axis) exhibits negligible net finite strain.

We now know several features in the bulk deformation which permit us to assume that it was probably caused by boundary conditions which can be closely approximated by the transpression tensor of Sanderson & Marchini (1984). These are listed as follows.
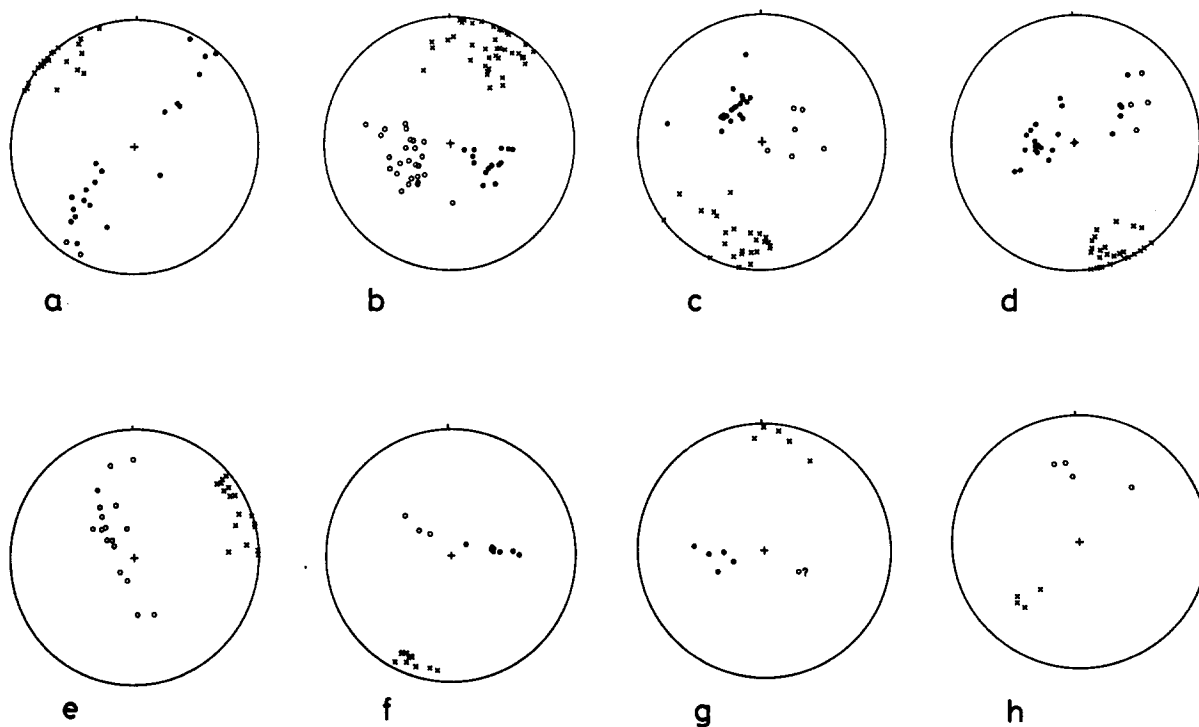

Fig. 11. Eight sets of faults identified in the mapped and adjacent parts of the southeast block of the Ardross Fault zone. Poles to the faults are shown as crosses. The map separations for different orientations of bedding are represented at the points of bedding–fault intersection. Open and solid circles denote sinistral and dextral separations, respectively. For a great circle spread, the slip vector lies between the two groups of symbols. (a) Steep dextral wrench faults, sub-parallel to the Ardross Fault (cf. the Y-shears of Bartlett *et al.* 1981). (b), (c) SSW and NNE-dipping normal faults. (d) Steep, oblique, normal-dextral wrench faults trending about 25° clockwise from the Ardross Fault, (cf. synthetic R-shears in transpression, see Sanderson & Marchini 1984, fig. 5). (e) Steep sinistral wrench faults conjugate to the R-shears. (f), (g) Steep NNE- and SSW-dipping reverse faults, possibly rotated and inverted equivalents of the more common normal faults which have this trend. (h) Others.
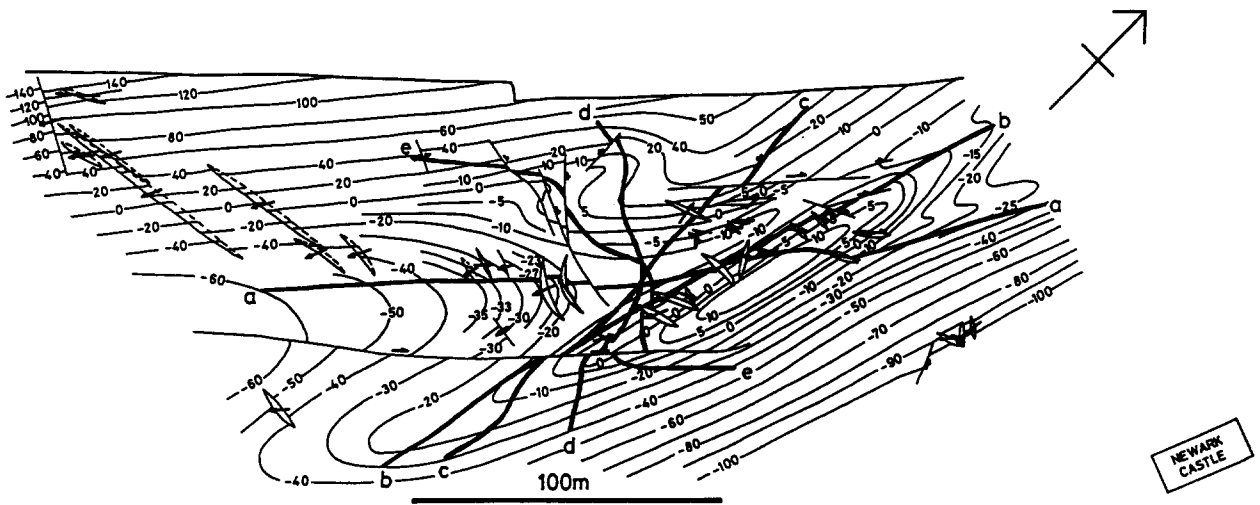
Fig. 12. The traces, a–e, of five segmented helices generated in different directions across the contour map shown in Fig. 10.

(1) The zone is bounded by a pair of steep and parallel boundary faults that are considerably longer than their normal separation. So for most points in the upper crustal portion of this block the nearest free surface will be vertically upwards.

(2) Horizontal fold axes with vertical axial surfaces trend at low acute angles from the boundary faults. These imply a significant vertical extension and a significant horizontal shortening oblique to the boundaries (normal to fold axes).

(3) Minor faults generally extend the traces of the fold axes, implying a significant horizontal lengthening oblique to the boundaries (parallel to fold axes).

(4) Although deformed, a horizontal line trending subparallel to the Ardross Fault shows negligible net finite strain.

From Fig. 13, knowledge of the orientation and dimensions of the sectional ellipse relative to the boundary fault (taken as the kinematic zx plane) enables the possible transpression tensor solutions to be examined. This is achieved by numerical substitution, as described above, and leads to the specification of the following 'best' transpression tensor D;

$$D = \begin{vmatrix} 1 & -0.38 & 0 \\ 0 & 0.56 & 0 \\ 0 & 0 & 1.78 \end{vmatrix}.$$

The orientations and magnitudes of the principal axes are determined by finding the eigenvectors and eigenvalues of the Finger tensor, DD' (Sanderson et al. 1980, Sanderson 1982). Such an analysis reveals that the ratio of the finite principal stretches, $s_1 : s_2 : s_3$ is 1.78 : 1.09 : 0.51 and the angle between the major axis of the horizontal sectional ellipse and the fault boundary, $\theta' = 13.7°$ (anticlockwise). The orientation of the minimum principal stretch (s_3) is sub-perpendicular to the fold axes and that of the maximum principal stretch (s_1) is vertical (sub-parallel to the axial planes). The maximum horizontal extension is sub-parallel to the axial traces and at a high angle to the extensional faults.

Figure 14 gives an impression of the size of the suite of probable transpression tensor solutions which can be
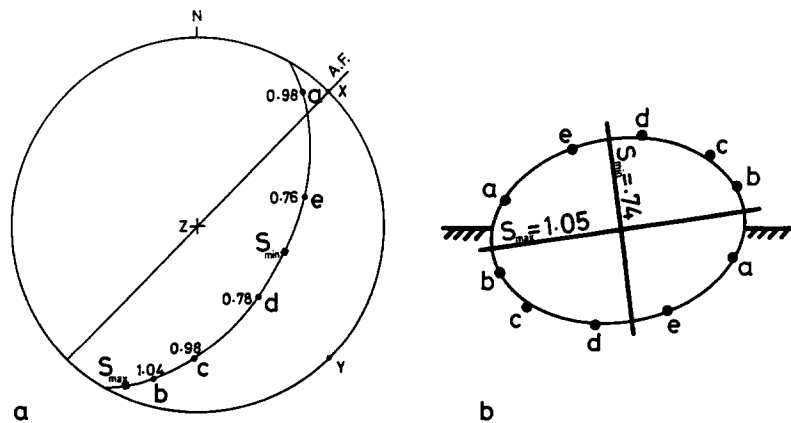

Fig. 13. (a) A stereogram depicting a great circle in the plane of regional bedding (50°/120°) with the stretches determined from Fig. 12 given in the appropriate orientations a–e. (b) The sectional strain ellipse in this inclined plane corresponding to these stretches. s_{max} and s_{min} are the maximum and minimum principal stretches of the inclined sectional ellipse. The cross-hatching denotes the attitude of a horizontal line. The co-ordinate axes (x, y, z) of the transpression tensor and the trend of the Ardross Fault (A.F.) are also shown.
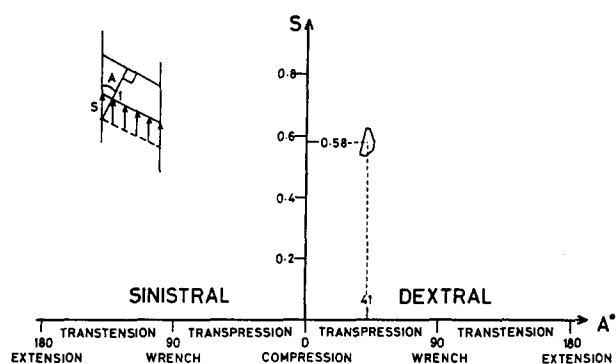
Fig. 14. A plot of S, the relative magnitude of zone-boundary displacement against A, the angle of boundary displacement (see inset for geometrical relationships). The nest of solutions centred on $S = 0.58$ and $A = 41°$ (dextral) are the possible transpressions, within certain error limits (see text), which satisfy the inclined sectional ellipse of Fig. 13.

Fig. 15. Restoration of the Ardross Fault when $S = 0.58$ and $A = 41°$ (dextral). F_0 is the relative position of the fault when the deformation is restored. F' is the present position of the fault and the dotted line is the SE margin of the restored, fault-parallel tract.

constrained by the sectional ellipse, when its principal axes are considered accurate to within ±10% and its orientation to within ±10°. The figure shows a plot of S, the magnitude of zone-boundary displacement, against A, the angle describing the obliquity of the deformation (see the inset in Fig. 14 for the precise geometrical relationships of S and A, and McCoss 1986 for the definitions of S and A in terms of the tensor components). It can be seen from this plot that the probable suite of solutions is compact and implies a dextral transpressional deformation with S approximately equal to 0.58 (relative to a zone of initial unit width) and A approximately 41°. (The angle A is defined as the horizontal angle between the displacement vector and the normal to the zone boundary.)

A restoration of these boundary conditions is depicted in Fig. 15 and suggests that the boundary displacement was relatively west to east. This is entirely compatible with the concept of Hercynian E–W compression in the Scottish Midland Valley, as implied by the N–S trending regional flexures and the contemporaneous E–W dyke swarms (Fig. 9). Furthermore, if D^{-1}, the reciprocal deformation is applied to a plane parallel to regional bedding (in which the strain measurements were made) then the plane in the deformed state (50°/120°) is rotated to dip 19°/104°. This too is compatible with independent geological evidence from the area, since this orientation of undeformed bedding is typical of that found outside the intensely deformed 1.5 km wide tract along the southeast side of the Ardross Fault, for example, in the gently ESE-dipping limb of the Anstruther Anticline.

Since the width of the studied zone is less than the width of the zone of deformation (due to the limit of exposure) it is important to note that this is only a partial restoration, for the rocks exposed on the foreshore. Hence the magnitude of zone-boundary displacement is an underestimate for the region as a whole. Furthermore the displacement vector may refract with distance from the fault, so the presented solution claims to be no more than that for a small homogeneously strained region nearest to the fault. Other studies, however, could
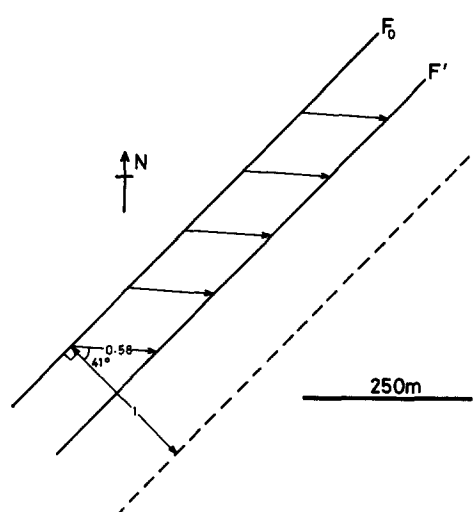
examine larger volumes of rock, since the techniques are essentially independent of scale.

CONCLUSIONS

Only in special cases, in which originally straight lines in bedding lie normal to horizontal fold axes and parallel to the map components of fault slip vectors (for their entire lengths), do lines deform to vertical planar faulted curves. These are the only cases for which sections containing them should be restored by either line or area balancing. In general, an originally straight line deforms to a segmented irregular helix, due to three-dimensional brittle and ductile translations and rotations of material. It is the length of the three-dimensional envelope bounding this segmented helix, divided by the sum of the lengths of the component helical fragments, which gives the true stretch. Methods have been presented in this paper which enable the traces of these segmented helices to be generated across structure contour maps. From the position on the map and the height from the contours the three-dimensional lengths can be measured and the stretch computed.

A technique has been devised to obtain the slip vectors from standard geological map data, namely bedding attitude, fault attitude and sense of map separation. In other situations slickenside lineations or piercements may be used to determine the slip vector. What is important however, is that slip vectors must be constrained if triaxial deformations are to be restored.

The consequences of folding must also be considered, and if helical loci are to be generated across structure contour maps then a folding model must be adopted. Flexural-slip represents one such simple fold model, which is frequently appropriate in non-metamorphic rocks. Any folding model could, however, be adopted, so long as the form of the locus of a deformed line can be

adequately defined. In the case of flexural-slip folds this locus, when plotted on a stereogram, is simply a partial small circle centred on the fold axis. Ideally, lineations in the field should be used to determine the true locus, but in non-metamorphic deformations these are generally rare so indirect methods have to be used to show that the model is compatible with the available data, for example, fold morphology and the characteristics of the strain (or lack of it) within bedding.

Having determined the stretches of initially straight lines in different directions within regional bedding, a least-squares bulk sectional strain ellipse can be determined. In general this measured finite strain cannot give a unique boundary solution; however it can if a probable deformation tensor is assumed. In this paper the transpression tensor of Sanderson & Marchini (1984) is adopted because it is general, simple, three-dimensional and can describe a spectrum of oblique deformations (McCoss 1986). This spectrum ranges continuously from plane strain in thrust belts through triaxial transpression, to simple shear in wrench zones, and from there through triaxial transtension to plane strain in extensional basins.

The methods have been applied to the Upper Viséan to Lower Namurian rocks adjacent to the Ardross Fault, a steep, NE-trending, Hercynian, dextral wrench fault in Fife, Scotland. The results indicate that, in response to Hercynian east–west shortening, the northwestern block was displaced relatively eastwards. This generated dextral transpression in the block bounded to the northwest by the Ardross Fault and to the southeast by the adjacent and parallel Firth of Forth Fault. The transpressional phase of the Ardross Fault must have ended by Stephanian to Permian times since relatively undeformed volcanic vents of this age cut the closely folded Upper Viséan to Lower Namurian sedimentary rocks.

The methods described in this paper could be used either directly or in modified form to suit other faulting, folding and deformation models. Furthermore, because the basic techniques are independent of scale, they could be applied to larger regions. Indeed studies at the scale of the example presented in this paper could be used to analyse the partitioning or compartmentalisation of strain within larger tectonic zones.

REFERENCES

Anderson, E. M. 1951. *The Dynamics of Faulting*. 2nd ed. Oliver and Boyd, Edinburgh and London.

Barr, D. 1984a. Geometric techniques for the palinspastic restoration of contoured geological horizons, with application to the Inner Moray Firth basin. *Rep. Br. geol. Surv.* ICSO/84/5 (Spatial Models).

Barr, D. 1984b. FORTRAN 77 programs for the palinspastic restoration of contoured geological horizons in extensional basins, with optional strain characteristics and depth to detachment determination. *Rep. Br. geol. Surv.* ICSO/84/6 (Spatial Models).

Barr, D. 1985. 3-D palinspastic restoration of normal faults in the Inner Moray Firth: implications for extensional basin development. *Earth Planet. Sci. Lett.* **75**, 191–203.

Bartlett, W. L., Friedman, M. & Logan, J. M. 1981. Experimental folding and faulting of rocks under confining pressure. *Tectonophysics* **79**, 255–277.

Cumming, G. A. 1936. The structural and volcanic geology of the Elie–St. Monance district, Fife. *Trans. geol. Soc. Edinb.* **13**, 340–365.

Forsyth, I. H. & Chisolm, J. I. 1968. Geological Survey bores in the Carboniferous of East Fife, 1963–1964. *Bull. geol. Surv. Gt Br.* **28**, 61–101.

Forsyth, I. H. & Rundle, C. C. 1978. The age of the volcanic and hypabyssal rocks of east Fife. *Bull. geol. Surv. Gt Br.* **60**, 23–29.

Francis, E. H. 1968. Pyroclastic and related rocks of the Geological Survey bores in East Fife, 1963–1964. *Bull. geol. Surv. Gt Br.* **28**, 121–135.

Francis, E. H. & Ewing, C. J. C. 1961. Coal Measures and volcanism off the Fife coast. *Geol. Mag.* **98**, 501–510.

Francis, E. H. & Hopgood, A. M. 1970. Volcanism and the Ardross Fault, Fife, Scotland. *Scott. J. Geol.* **6**, 162–185.

Geikie, A. 1879. The Carboniferous rocks of the Basin of the Forth. *Trans. R. Soc. Edinb.* **29**, 437–518.

Geikie, A. 1902. The geology of eastern Fife. *Mem. geol. Surv. Gt Br.*

Gill, P. E. & Murray, W. 1978. Algorithms for the solution of non-linear least squares problem. *Soc. ind. appl. Math. J. numer. Anal.* **15**, 977–992.

McCoss, A. M. 1986. Simple constructions for deformation in transpression/transtension zones. *J. Struct. Geol.* **8**, 715–718.

McCoss, A. M. 1987. Practical section drawing through folded layers using sequentially rotated cubic interpolators. *J. Struct. Geol.* **9**, 365–370.

Ramsay, J. G. 1967. *Folding and Fracturing of Rocks*. McGraw-Hill, New York.

Sanderson, D. J., Andrews, J. R., Phillips, W. E. A. & Hutton, D. H. W. 1980. Deformation studies in the Irish Caledonides. *J. geol. Soc. Lond.* **137**, 289–302.

Sanderson, D. J. 1982. Models of strain variation in nappes and thrust sheets: a review. *Tectonophysics* **88**, 201–233.

Sanderson, D. J. & Marchini, W. R. D. 1984. Transpression. *J. Struct. Geol.* **6**, 449–458.